

On an Improved Unusual Stabilized Finite Element Method for the Advective-Reactive-Diffusive Equation

L. P. Franca

Department of Mathematics
University of Colorado at Denver
P.O. Box 17364, Campus Box 170
Denver, CO 80217-3364, USA

and

F. Valentin*

Laboratório Nacional de Computação Científica - LNCC
Avenida Gétúlio Vargas, 333
Quitandinha, Caixa Postal 95113
25651-070 Petrópolis - RJ, BRAZIL

April 28, 1999

Abstract

An improved unusual finite element method is studied herein for a second-order linear scalar differential equation including a zero order term. The method consists in subtracting from the standard Galerkin method a mesh dependent term suggested by static condensation of the bubbles. Based on this idea, a new stabilized parameter is constructed, which improves accuracy of the solution. Several numerical tests attest the efficiency of the present method and an error analysis is performed.

*The work of this author was supported by Conselho Nacional de Pesquisas (CNPq) - Brazil and Institut National de Recherche en Informatique et en Automatique (INRIA-Rocquencourt) - France

1 Introduction

Stabilized finite elements have been around for more than 20 years now, starting with the SUPG method introduced by Hughes and Brooks [3, 12]. These methods have the desirable properties of improving the numerical stability of the Galerkin method and of preserving good accuracy properties. Variations of this idea were considered for the advective-diffusive equation: the Galerkin-least-squares version was introduced in 1989 in [13], and a few years later, an unusual version was termed stabilized methods [7, 6].

It is well known that the Galerkin method using low order piecewise polynomials perform poorly for advection-dominated equations. Adding terms to the variational formulation is a well accepted practice, as it is done using stabilized methods. It was rather unexpected that the Galerkin method without additional terms can be used as a starting point for these problems as well. In [1] a relationship is established between the Galerkin method enriched with bubble functions and the stabilized method of [7] for advective-diffusive equations. If we take inappropriate choices of bubbles, then the Galerkin method will perform as a disguised stabilized method with the wrong selection of the stability parameter. To treat this pathology, special bubble designs were suggested [1, 14, 2, 9]. Among them, residual-free bubbles take into account the partial differential equation being approximated, in the generation of the enrichment space being added to the finite element piecewise polynomial space. Although residual-free bubbles form a framework to derive improved discretizations, we still need to compute residual-free basis functions by solving strongly partial differential equations at the element level. Progress has been made in approximating these computations [8], but in this work we will circumvent these difficulties by pursuing an improved unusual stabilized method (USFEM) in the form as given in [6]. Herein, we use a mesh parameter inspired by residual-free bubbles, as part of the new stability parameter design that we introduce in this work.

The purpose of this work is to demonstrate that improved numerical results can be attained with the unusual stabilized method [6] for advective-reactive-diffusive equations, by carefully revisiting the definition of the stability parameter. In [6], the stability parameter design was considered by looking at the asymptotic behavior of the solution of the second order linear equation, including a zero order term, and by looking at the global convergence error analysis to check whether smooth solutions would converge at desirable rates. However, in the presence of advection, in the case of a large zero order term, the unusual stabilized method [6] does not perform well, and this has led us to revisit the design of the stability parameter for this method.

In this paper, we use USFEM as the starting point and by looking at three asymptotic limits (for high advection, diffusion and reaction), we design a newer parameter that has superior numerical performance and preserve the global convergence error estimates rates that were obtained before [7, 6].

In Section 2 we present the formulation along with the new design of the stability parameter. In Section 3 a global convergence analysis is performed and in Section 4 numerical experiments confirm the improvement of accuracy over the previous ver-

sions of this method.

2 Stabilized method for the model problem

The linear advective-reactive-diffusive model is governed by the following boundary value problem:

$$\begin{cases} \sigma u + \mathbf{a} \cdot \nabla u - \nu \Delta u = f & \text{in } \Omega, \\ u = 0 & \text{on } \Gamma, \end{cases} \quad (1)$$

where u is the unknown scalar variable (e.g., temperature); σ and ν are given positive coefficients representing reactive and diffusivity parameters, respectively; \mathbf{a} is the given velocity field; f is the source and $\Omega \subset \mathbb{R}^2$ is an open bounded domain with smooth boundary $\Gamma = \partial\Omega$. The variational formulation corresponding to (1) is: find $u \in H_0^1(\Omega)$ such that

$$(\sigma u, v) + (\mathbf{a} \cdot \nabla u, v) + (\nu \nabla u, \nabla v) = (f, v), \quad \forall v \in H_0^1(\Omega). \quad (2)$$

The standard Galerkin method consists in choosing a subspace $V_h \subset H_0^1(\Omega)$ and solving the following problem: Find $u_h \in V_h$ such that

$$(\sigma u_h, v_h) + (\mathbf{a} \cdot \nabla u_h, v_h) + (\nu \nabla u_h, \nabla v_h) = (f, v_h), \quad \forall v_h \in V_h. \quad (3)$$

It is well known that for a subspace spanned by piecewise linear elements, this formulation yields poor approximations when $\nu \ll |\mathbf{a}|$ or when $\nu \ll \sigma$. In this paper, we propose to improve an unusual stabilized method introduced in [6]. The method can be written as:

Find $u_h \in V_h$ such that

$$B(u_h, v_h) = F(v_h), \quad \forall v_h \in V_h, \quad (4)$$

where

$$\begin{aligned} B(u, v) &= (\sigma u, v) + (\mathbf{a} \cdot \nabla u, v) + (\nu \nabla u, \nabla v) \\ &\quad - \sum_{K \in \mathcal{C}_h} (\sigma u + \mathbf{a} \cdot \nabla u - \nu \Delta u, \tau_K (\sigma v - \mathbf{a} \cdot \nabla v - \nu \Delta v))_K \end{aligned} \quad (5)$$

and

$$F(v) = (f, v) - \sum_{K \in \mathcal{C}_h} (f, \tau_K (\sigma v - \mathbf{a} \cdot \nabla v - \nu \Delta v))_K. \quad (6)$$

We introduce a new stability parameter, given by:

$$\tau_K = \frac{h_K^2}{\sigma h_K^2 \xi (Pe_K^1(\mathbf{x})) + \frac{2\nu}{m_k} \xi (Pe_K^2(\mathbf{x}))}, \quad (7)$$

$$Pe_K^1(\mathbf{x}) = \frac{2\nu}{m_k \sigma h_K^2}, \quad (8)$$

$$Pe_K^2(\mathbf{x}) = \frac{m_k |\mathbf{a}(\mathbf{x})|_p h_K}{\nu}, \quad (9)$$

$$\xi(\mathbf{x}) = \begin{cases} 1 & , \quad 0 \leq \mathbf{x} < 1, \\ \mathbf{x} & , \quad \mathbf{x} \geq 1, \end{cases} \quad (10)$$

$$|\mathbf{a}(\mathbf{x})|_p = \left(\sum_{i=1}^N |a_i(\mathbf{x})|^p \right)^{1/p}, \quad 1 \leq p < \infty, \quad (11)$$

$$C_K \sum_{K \in \mathfrak{S}_h} h_K^2 \|\Delta v\|_{0,K}^2 \leq \|\nabla v\|_0^2, \quad \forall v \in V_h, \quad (12)$$

$$m_k = \min \left\{ \frac{1}{3}, C_K \right\}. \quad (13)$$

Remarks:

1. The formula for τ_K has a form that is suggested by static condensation, as explained in [6], along with two switches for the asymptotic behavior of the coefficients σ , $|\mathbf{a}|$ and ν . The comparison between these coefficients are performed by the different Pe_K^i and the final parameter τ_K reflects the asymptotic behavior under any limiting case. Removing the switches the formula is similar to the parameter proposed in [5].
2. We have found that, under the presence of advection ($\mathbf{a} \neq \mathbf{0}$), the element parameter h_K that yields the best numerical results is computed using the largest streamline distance in the element. Illustration on how this distance is computed can be found in figure 1. The computation of h_K using this idea is suggested by residual-free-bubbles (e.g., see [9] and references therein).

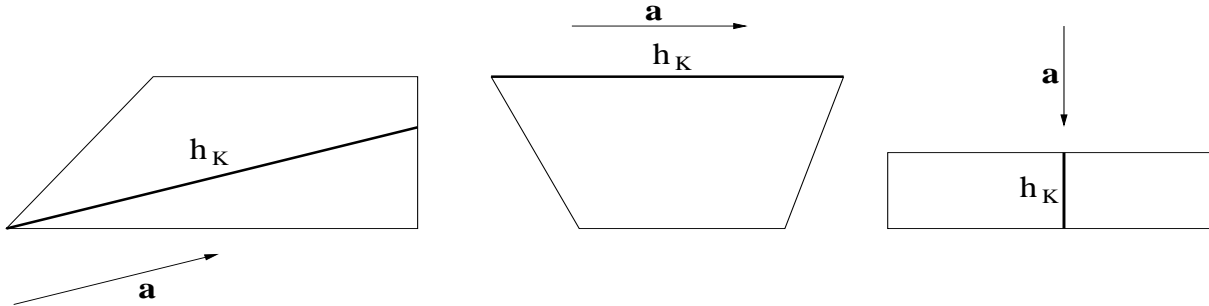


Figure 1: The element parameter computation.

3 Error analysis

Let us first consider the numerical stability of this method. Denoting by

$$\alpha_K = \frac{\nu}{m_k \sigma h_K^2 + 2\nu},$$

we can establish:

Lemma 1

Let us assume that $\mathbf{a} \in H^1(\Omega) \cap L^\infty(\Omega)$ and the given data satisfy:

- i) $\nabla \cdot \mathbf{a} = 0$ in Ω ,
- ii) $\nu(\mathbf{x}) = \nu = \text{const} > 0$ in Ω ,
- iii) $\sigma(\mathbf{x}) = \sigma = \text{const} > 0$ in Ω .

Then $\forall u_h \in V_h$ we have

$$B(u_h, u_h) \geq \sum_{K \in C_h} \left(\sigma \alpha_K \|u_h\|_{0,K}^2 + \nu \alpha_K \|\nabla u_h\|_{0,K}^2 + \tau_K \|\mathbf{a} \cdot \nabla u_h\|_{0,K}^2 \right) \quad (14)$$

Proof :

An upper bound for τ_K follows by (7)-(13). From (10), $\xi \geq 1$, and, therefore, for each element we have:

$$\tau_K \leq \frac{m_k h_K^2}{m_k \sigma h_K^2 + 2\nu}, \quad (15)$$

and by definition of m_k , it follows that $m_k \leq C_K$.

Taking $v = u_h$ in (1) and using (15) we have:

$$\begin{aligned} & B(u_h, u_h) \\ &= \sigma \|u_h\|^2 + \nu \|\nabla u_h\|^2 + \sum_{K \in C_h} \tau_K \left(-\sigma^2 \|u_h\|_{0,K}^2 + \|\mathbf{a} \cdot \nabla u_h\|_{0,K}^2 + 2\sigma \nu (u_h, \Delta u_h)_{0,K} - \nu^2 \|\Delta u_h\|_{0,K}^2 \right) \\ &\geq \sum_{K \in C_h} \left(\left(\sigma - \frac{m_k h_K^2 \sigma^2}{m_k \sigma h_K^2 + 2\nu} - \frac{m_k \nu \sigma h_K^2}{\gamma (m_k \sigma h_K^2 + 2\nu)} \right) \|u_h\|_{0,K}^2 \right. \\ &\quad \left. + \left(\nu - \frac{\nu^2}{m_k \sigma h_K^2 + 2\nu} - \frac{\gamma \nu \sigma}{m_k \sigma h_K^2 + 2\nu} \right) \|\nabla u_h\|_{0,K}^2 \right. \\ &\quad \left. + \tau_K \|\mathbf{a} \cdot \nabla u_h\|_{0,K}^2 \right) \\ &= \sum_{K \in C_h} \left(\frac{\sigma \nu (2\gamma - m_k h_K^2)}{\gamma (m_k \sigma h_K^2 + 2\nu)} \|u_h\|_{0,K}^2 + \frac{\nu^2 + \sigma \nu (m_k h_K^2 - \gamma)}{m_k \sigma h_K^2 + 2\nu} \|\nabla u_h\|_{0,K}^2 \right. \\ &\quad \left. + \tau_K \|\mathbf{a} \cdot \nabla u_h\|_{0,K}^2 \right), \end{aligned}$$

and the result follows choosing $\gamma = m_k h_K^2$ in each element K .

□

Let k be an integer with $k \geq 1$. We suppose the existence of an interpolation operator $I_h : V \rightarrow V_h$ (see [4]) such that the approximation of u by $\tilde{u}_h = I_h u$ can be estimated as following:

$$\|u - \tilde{u}_h\|_{m,K} \leq C h_K^{l-m} \|u\|_{l,K}, \quad u \in H^l(K), \quad (16)$$

$0 \leq m \leq 2$ and $\max\{m, 1\} \leq l \leq k + 1$

The following interpolation estimate can now be established.

Lemma 2

Assume that the solution of (2) satisfies $u \in H^{k+1}(\Omega) \cap H_0^1(\Omega)$. Denoting by $\eta = u - \tilde{u}_h$ the interpolation error, for each $K \in \mathcal{C}_h$:

a) if $Pe_K^1(\mathbf{x}) \geq 1$ and $Pe_K^2(\mathbf{x}) < 1$, $\forall \mathbf{x} \in K$, then

$$\begin{aligned} & \nu \|\nabla \eta\|_{0,K}^2 + \frac{\sigma}{\alpha_K} \|\eta\|_{0,K}^2 + \frac{1}{\sigma \alpha_K} \|\mathbf{a} \cdot \nabla \eta\|_{0,K}^2 + \frac{\nu^2}{\sigma \alpha_K} \|\Delta \eta\|_{0,K}^2 \\ & \leq C \nu h_K^{2k} \|u\|_{k+1,K}^2 \end{aligned}$$

b) if $Pe_K^1(\mathbf{x}) \geq 1$ and $Pe_K^2(\mathbf{x}) \geq 1$, $\forall \mathbf{x} \in K$, then

$$\begin{aligned} & \nu \|\nabla \eta\|_{0,K}^2 + \frac{\sigma}{\alpha_K} \|\eta\|_{0,K}^2 + \frac{1}{\sigma \alpha_K} \|\mathbf{a} \cdot \nabla \eta\|_{0,K}^2 + \frac{\nu^2}{\sigma \alpha_K} \|\Delta \eta\|_{0,K}^2 \\ & \leq C \sup |\mathbf{a}|_p h_K^{2k+1} \|u\|_{k+1,K}^2 \end{aligned}$$

c) if $Pe_K^1(\mathbf{x}) < 1$ and $Pe_K^2(\mathbf{x}) < 1$, $\forall \mathbf{x} \in K$, then

$$\begin{aligned} & \nu \|\nabla \eta\|_{0,K}^2 + \frac{\sigma}{\alpha_K} \|\eta\|_{0,K}^2 + \frac{1}{\sigma \alpha_K} \|\mathbf{a} \cdot \nabla \eta\|_{0,K}^2 + \frac{\nu^2}{\sigma \alpha_K} \|\Delta \eta\|_{0,K}^2 \\ & \leq C \sigma h_K^{2k+2} \|u\|_{k+1,K}^2 \end{aligned}$$

d) if $Pe_K^1(\mathbf{x}) < 1$ and $Pe_K^2(\mathbf{x}) \geq 1$, $\forall \mathbf{x} \in K$, then

$$\begin{aligned} & \nu \|\nabla \eta\|_{0,K}^2 + \frac{\sigma}{\alpha_K} \|\eta\|_{0,K}^2 + \frac{1}{\sigma \alpha_K} \|\mathbf{a} \cdot \nabla \eta\|_{0,K}^2 + \frac{\nu^2}{\sigma \alpha_K} \|\Delta \eta\|_{0,K}^2 \\ & \leq C h_K^{2k+1} \max\{\sup |\mathbf{a}|_p, \sigma h_K\} \|u\|_{k+1,K}^2 \end{aligned}$$

Therefore,

$$\begin{aligned}
& \nu \|\nabla \eta\|_0^2 + \sum_{K \in \mathcal{C}_h} \left(\frac{\sigma}{\alpha_K} \|\eta\|_{0,K}^2 + \frac{1}{\sigma \alpha_K} \|\mathbf{a} \cdot \nabla \eta\|_{0,K}^2 + \frac{\nu^2}{\sigma \alpha_K} \|\Delta \eta\|_{0,K}^2 \right) \\
& \leq C \sum_{K \in \mathcal{C}_h} h_K^{2k} \|u\|_{k+1,K}^2 \left(H(Pe_K^1 - 1) H(1 - Pe_K^2) \nu \right. \\
& \quad \left. + H(Pe_K^1 - 1) H(Pe_K^2 - 1) \sup |\mathbf{a}|_p h_K + H(1 - Pe_K^1) H(1 - Pe_K^2) \sigma h_K^2 \right. \\
& \quad \left. + H(1 - Pe_K^1) H(Pe_K^2 - 1) \max\{\sup |\mathbf{a}|_p h_K, \sigma h_K^2\} \right)
\end{aligned}$$

Proof:

We divide the proof in four parts:

a) Let $Pe_K^1(\mathbf{x}) \geq 1$ and $Pe_K^2(\mathbf{x}) \leq 1$, $\forall \mathbf{x} \in K$.

Let us first note that

$$\frac{1}{\alpha_K} = \frac{\frac{2\nu}{Pe_K^1} + 2\nu}{\nu} \leq 4.$$

Then,

$$\begin{aligned}
& \nu \|\nabla \eta\|_{0,K}^2 + \frac{\sigma}{\alpha_K} \|\eta\|_{0,K}^2 + \frac{1}{\sigma \alpha_K} \|\mathbf{a} \cdot \nabla \eta\|_{0,K}^2 + \frac{\nu^2}{\sigma \alpha_K} \|\Delta \eta\|_{0,K}^2 \\
& \leq C \left(\nu \|\nabla \eta\|_{0,K}^2 + \sigma \|\eta\|_{0,K}^2 + \|\sigma^{-1/2} |\mathbf{a}|_p \cdot |\nabla \eta|_2\|_{0,K}^2 + \frac{\nu^2}{\sigma} \|\Delta \eta\|_{0,K}^2 \right) \\
& \leq C \left(\nu \|\nabla \eta\|_{0,K}^2 + \frac{2\nu}{Pe_K^1 m_k h_K^2} \|\eta\|_{0,K}^2 + \left\| \sqrt{\frac{m_k h_K^2 Pe_K^1}{2\nu} \frac{\nu Pe_K^2}{m_k h_K}} |\nabla \eta|_2 \right\|_{0,K}^2 \right. \\
& \quad \left. + \frac{\nu m_k h_K^2 Pe_K^1}{2} \|\Delta \eta\|_{0,K}^2 \right) \\
& \leq C \left(\nu \|\nabla \eta\|_{0,K}^2 + \nu h_K^{-2} \|\eta\|_{0,K}^2 + \nu h_K^2 \|\Delta \eta\|_{0,K}^2 \right) \\
& \leq C \nu h_K^{2k} \|u\|_{k+1,K}^2.
\end{aligned}$$

b) Let $Pe_K^1(\mathbf{x}) \geq 1$ and $Pe_K^2(\mathbf{x}) \geq 1$, $\forall \mathbf{x} \in K$.

Let us first note that

$$\frac{1}{\alpha_K} = \frac{\frac{2m_k |\mathbf{a}|_p h_K}{Pe_K^2 Pe_K^1} + \frac{2m_k |\mathbf{a}|_p h_K}{Pe_K^2}}{\frac{m_k |\mathbf{a}|_p h_K}{Pe_K^2}} \leq 4.$$

Then,

$$\begin{aligned}
& \nu \|\nabla \eta\|_{0,K}^2 + \frac{\sigma}{\alpha_K} \|\eta\|_{0,K}^2 + \frac{1}{\sigma \alpha_K} \|\mathbf{a} \cdot \nabla \eta\|_{0,K}^2 + \frac{\nu^2}{\sigma \alpha_K} \|\Delta \eta\|_{0,K}^2 \\
& \leq C \left(\nu \|\nabla \eta\|_{0,K}^2 + \sigma \|\eta\|_{0,K}^2 + \|\sigma^{-1/2} |\mathbf{a}|_p \cdot |\nabla \eta|_2\|_{0,K}^2 + \frac{\nu^2}{\sigma} \|\Delta \eta\|_{0,K}^2 \right) \\
& \leq C \left(\frac{m_k |\mathbf{a}|_p h_K}{Pe_K^2} \|\nabla \eta\|_{0,K}^2 + \frac{2 |\mathbf{a}|_p}{Pe_K^2 Pe_K^1 h_K} \|\eta\|_{0,K}^2 + \left\| \sqrt{\frac{h_K Pe_K^2 Pe_K^1}{2 |\mathbf{a}|_p}} |\mathbf{a}|_p |\nabla \eta|_2 \right\|_{0,K}^2 \right. \\
& \quad \left. + \frac{m_k^2 |\mathbf{a}|_p h_K^3 Pe_K^1}{2 Pe_K^2} \|\Delta \eta\|_{0,K}^2 \right) \\
& \leq C \left(\sup |\mathbf{a}|_p h_K \|\nabla \eta\|_{0,K}^2 + \sup |\mathbf{a}|_p h_K^{-1} \|\eta\|_{0,K}^2 + \sup |\mathbf{a}|_p h_K^3 \|\Delta \eta\|_{0,K}^2 \right) \\
& \leq C \sup |\mathbf{a}|_p h_K^{2k+1} \|u\|_{k+1,K}^2.
\end{aligned}$$

c) Let $Pe_K^1(\mathbf{x}) < 1$ and $Pe_K^2(\mathbf{x}) < 1$, $\forall \mathbf{x} \in K$.

Let us first note that

$$\frac{1}{\alpha_K} = \frac{m_k \sigma h_K^2 + Pe_K^1 m_k \sigma h_K^2}{\frac{Pe_K^1 m_k \sigma h_K^2}{2}} \leq \frac{2}{Pe_K^1} + 2 \leq \frac{4}{Pe_K^1}.$$

Then,

$$\begin{aligned}
& \nu \|\nabla \eta\|_{0,K}^2 + \frac{\sigma}{\alpha_K} \|\eta\|_{0,K}^2 + \frac{1}{\sigma \alpha_K} \|\mathbf{a} \cdot \nabla \eta\|_{0,K}^2 + \frac{\nu^2}{\sigma \alpha_K} \|\Delta \eta\|_{0,K}^2 \\
& \leq C \left(\nu \|\nabla \eta\|_{0,K}^2 + \sigma \|\eta\|_{0,K}^2 + \|\sigma^{-1/2} |\mathbf{a}|_p \cdot |\nabla \eta|_2\|_{0,K}^2 + \frac{\nu^2}{\sigma} \|\Delta \eta\|_{0,K}^2 \right) \\
& \leq C \left(\frac{m_k \sigma h_K^2 Pe_K^1}{2} \|\nabla \eta\|_{0,K}^2 + \sigma \|\eta\|_{0,K}^2 + \|\sigma^{-1/2} \frac{\sigma h_K Pe_K^2 Pe_K^1}{2} |\nabla \eta|_2\|_{0,K}^2 \right. \\
& \quad \left. + \frac{m_k^2 \sigma h_K^4 Pe_K^1}{4} \|\Delta \eta\|_{0,K}^2 \right) \\
& \leq C \left(\sigma h_K^2 \|\nabla \eta\|_{0,K}^2 + \sigma \|\eta\|_{0,K}^2 + \sigma h_K^4 \|\Delta \eta\|_{0,K}^2 \right) \\
& \leq C \sigma h_K^{2k+2} \|u\|_{k+1,K}^2.
\end{aligned}$$

d) Let $Pe_K^1(\mathbf{x}) < 1$ and $Pe_K^2(\mathbf{x}) \geq 1$, $\forall \mathbf{x} \in K$.

Using the relation $\sigma = \frac{2|\mathbf{a}|_p}{h_K Pe_K^2 Pe_K^1}$ the result for $\sup |\mathbf{a}|_p \geq \sigma h_K$ is reached from the same way as in item (b) and as in item (c) otherwise, and the result follows.

□

We will now establish the convergence estimate.

Theorem 3

Under the hypotheses of Lemmas 1 and 2, the solution u_h of the method given by (4) converges to u , solution of (2) as follows:

$$\begin{aligned} & \sigma \|u_h - u\|_0^2 + \nu \|\nabla(u_h - u)\|_0^2 + \sum_{K \in C_h} \tau_K \|\mathbf{a} \cdot \nabla(u_h - u)\|_{0,K}^2 \\ & \leq C \sum_{K \in C_h} h_K^{2k} \|u\|_{k+1,K}^2 (H(Pe_K^1 - 1)H(1 - Pe_K^2)\nu \\ & \quad + H(Pe_K^1 - 1)H(Pe_K^2 - 1)\sup |\mathbf{a}|_p h_K + H(1 - Pe_K^1)H(1 - Pe_K^2)\sigma h_K^2 \\ & \quad + H(1 - Pe_K^1)H(Pe_K^2 - 1)\max\{\sup |\mathbf{a}|_p h_K, \sigma h_K^2\}) \end{aligned}$$

Proof:

Let $e_h = u_h - \tilde{u}_h$ and $e = e_h + \eta$. Then

$$\begin{aligned} & \sum_{K \in C_h} \left(\sigma \alpha_K \|e_h\|_{0,K}^2 + \nu \alpha_K \|\nabla e_h\|_{0,K}^2 + \tau_K \|\mathbf{a} \cdot \nabla e_h\|_{0,K}^2 \right) \\ & \leq B(e_h, e_h) \\ & = B(e - \eta, e_h) \\ & = -B(\eta, e_h) \\ & = -\sigma(\eta, e_h) - (\mathbf{a} \cdot \nabla \eta, e_h) - \nu(\nabla \eta, \nabla e_h) + \sum_{K \in C_h} \tau_K (\sigma \eta + \mathbf{a} \cdot \nabla \eta - \nu \Delta \eta, \sigma e_h - \mathbf{a} \cdot \nabla e_h - \nu \Delta e_h)_K \\ & = \sum_{K \in C_h} \left(\sigma(1 - \sigma \tau_K) \left(\frac{-\sigma \eta - \mathbf{a} \cdot \nabla \eta + \nu \Delta \eta}{\sigma}, e_h \right) + \tau_K (-\sigma \eta - \mathbf{a} \cdot \nabla \eta + \nu \Delta \eta, \mathbf{a} \cdot \nabla e_h) \right. \\ & \quad \left. + \tau_K (-\sigma \eta - \mathbf{a} \cdot \nabla \eta + \nu \Delta \eta, \nu \Delta e_h) \right) \\ & \leq C \sum_{K \in C_h} \left(\frac{1 - \sigma \tau_K}{\sigma} \|\sigma \eta + \mathbf{a} \cdot \nabla \eta - \nu \Delta \eta\|_{0,K}^2 + 2\tau_K \|\sigma \eta + \mathbf{a} \cdot \nabla \eta - \nu \Delta \eta\|_{0,K}^2 \right)^{1/2} \end{aligned}$$

$$\begin{aligned}
& (\sigma (1 - \sigma\tau_K) \|e_h\|_{0,K}^2 + \tau_K \|\mathbf{a} \cdot \nabla e_h\|_{0,K}^2 + \tau_K \nu^2 \|\Delta e_h\|_{0,K}^2)^{1/2} \\
\leq & C \sum_{K \in \mathcal{C}_h} \left(\frac{\alpha_K + \sigma\tau_K}{\sigma} \|\sigma\eta + \mathbf{a} \cdot \nabla \eta - \nu \Delta \eta\|_{0,K}^2 \right)^{1/2} \\
& (\sigma\alpha_K \|e_h\|_{0,K}^2 + \tau_K \|\mathbf{a} \cdot \nabla e_h\|_{0,K}^2 + \nu\alpha_K \|\nabla e_h\|_{0,K}^2)^{1/2}
\end{aligned}$$

Dividing by the last bracket terms, we have:

$$\begin{aligned}
& \sum_{K \in \mathcal{C}_h} (\sigma\alpha_K \|e_h\|_{0,K}^2 + \nu\alpha_K \|\nabla e_h\|_{0,K}^2 + \tau_K \|\mathbf{a} \cdot \nabla e_h\|_{0,K}^2)^{1/2} \\
\leq & C \sum_{K \in \mathcal{C}_h} \left(\frac{\alpha_K + \sigma\tau_K}{\sigma} \|\sigma\eta + \mathbf{a} \cdot \nabla \eta - \nu \Delta \eta\|_{0,K}^2 \right)^{1/2}
\end{aligned}$$

Squaring and dividing by α_K , we obtain:

$$\begin{aligned}
& \sigma \|e_h\|_0^2 + \nu \|\nabla e_h\|_0^2 + \sum_{K \in \mathcal{C}_h} \frac{\tau_K}{\alpha_K} \|\mathbf{a} \cdot \nabla e_h\|_{0,K}^2 \\
\leq & C \sum_{K \in \mathcal{C}_h} \frac{\alpha_K + \sigma\tau_K}{\sigma\alpha_K} (\|\sigma\eta\|_{0,K}^2 + \|\mathbf{a} \cdot \nabla \eta\|_{0,K}^2 + \|\nu \Delta \eta\|_{0,K}^2) \\
\leq & C \sum_{K \in \mathcal{C}_h} \left(\frac{\sigma}{\alpha_K} \|\eta\|_{0,K}^2 + \frac{1}{\sigma\alpha_K} \|\mathbf{a} \cdot \nabla \eta\|_{0,K}^2 + \frac{\nu^2}{\sigma\alpha_K} \|\Delta \eta\|_{0,K}^2 \right)
\end{aligned}$$

By triangle inequality and Lemma 2 we have:

$$\begin{aligned}
& \sigma \|e\|_0^2 + \nu \|\nabla e\|_0^2 + \sum_{K \in \mathcal{C}_h} \frac{\tau_K}{\alpha_K} \|\mathbf{a} \cdot \nabla e\|_{0,K}^2 \\
\leq & C \left(\sigma \|e_h\|_0^2 + \nu \|\nabla e_h\|_0^2 + \sum_{K \in \mathcal{C}_h} \frac{\tau_K}{\alpha_K} \|\mathbf{a} \cdot \nabla e_h\|_{0,K}^2 + \sigma \|\eta\|_0^2 + \nu \|\nabla \eta\|_0^2 + \sum_{K \in \mathcal{C}_h} \frac{\tau_K}{\alpha_K} \|\mathbf{a} \cdot \nabla \eta\|_{0,K}^2 \right) \\
= & C \sum_{K \in \mathcal{C}_h} \left(\sigma \frac{\alpha_K + 1}{\alpha_K} \|\eta\|_{0,K}^2 + \nu \|\nabla \eta\|_0^2 + \frac{1 + \sigma\tau_K}{\sigma\alpha_K} \|\mathbf{a} \cdot \nabla \eta\|_{0,K}^2 + \frac{\nu^2}{\sigma\alpha_K} \|\Delta \eta\|_{0,K}^2 \right) \\
\leq & C \sum_{K \in \mathcal{C}_h} \left(\frac{\sigma}{\alpha_K} \|\eta\|_{0,K}^2 + \nu \|\nabla \eta\|_0^2 + \frac{1}{\sigma\alpha_K} \|\mathbf{a} \cdot \nabla \eta\|_{0,K}^2 + \frac{\nu^2}{\sigma\alpha_K} \|\Delta \eta\|_{0,K}^2 \right) \\
\leq & C \sum_{K \in \mathcal{C}_h} h_K^{2k} \|u\|_{k+1,K}^2 (H (Pe_K^1 - 1) H (1 - Pe_K^2) \nu \\
& + H (Pe_K^1 - 1) H (Pe_K^2 - 1) \sup |\mathbf{a}|_p h_K + H (1 - Pe_K^1) H (1 - Pe_K^2) \sigma h_K^2)
\end{aligned}$$

$$+H(1 - Pe_K^1) H(Pe_K^2 - 1) \max\{\sup |\mathbf{a}|_p h_K, \sigma h_K^2\}$$

□

4 Numerical experiments

In this section we report four series of experiments with the unusual stabilized method in [6] using the new stability parameter design introduced in Section 2. In the following numerical results we illustrate the applicability of the method for different values of the coefficients, mainly for singularly perturbed problems, when we employ low values for diffusivity ν associated to high values of advection and/or reaction coefficients. Thereby, we are interested in the study of the accuracy of the method in solving complex problems in non-uniform meshes.

4.1 A reactive-diffusive problem:

First we simulate the problem described in Figure 2, in the absence of the advection term ($\mathbf{a} = \mathbf{0}$), with $\sigma = 1$, $\nu = 10^{-6}$ and $f = 1$. The unit square domain is partitioned into a uniform mesh with 441 nodes of triangles or quadrilaterals, depending whether we test piecewise linear or bilinear elements. In Figure 3 we verify that for both linear and bilinear elements, the spurious oscillations of the standard Galerkin method are eliminated. The numerical results are more accurate than the results of this method with the stability parameter as proposed in [6], as we can see from Figure 4. For this case, the stabilized method is related to the formulation studied by Harari and Hughes [10].

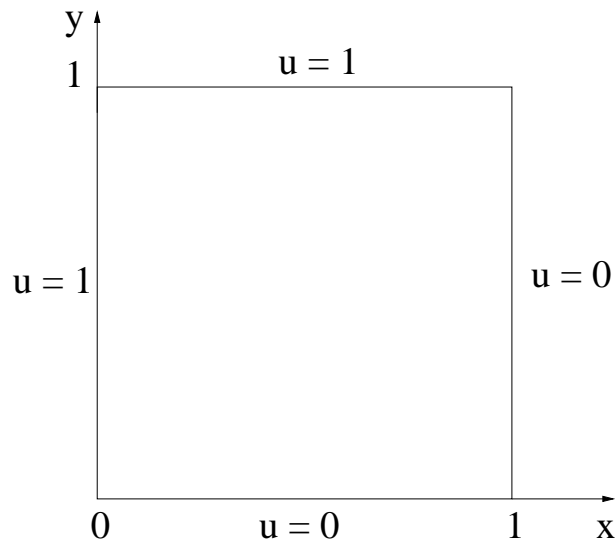
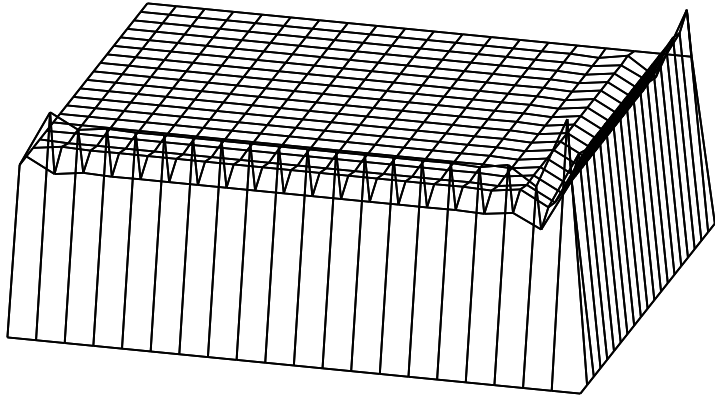
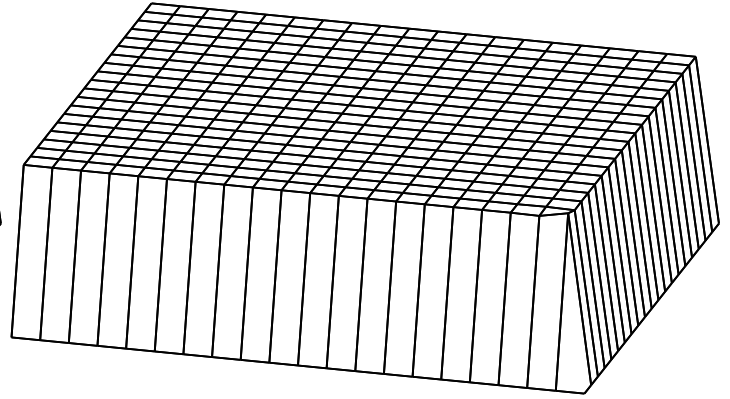


Figure 2: Reactive-diffusive problem.

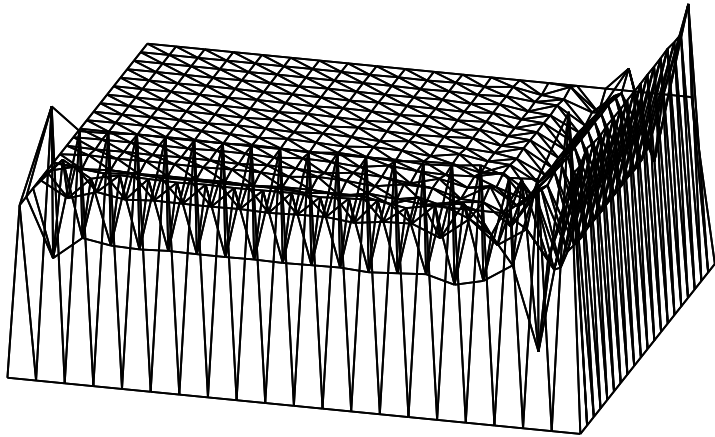
GALERKIN METHOD - Q1



PRESENT METHOD - Q1



GALERKIN METHOD - P1



PRESENT METHOD - P1

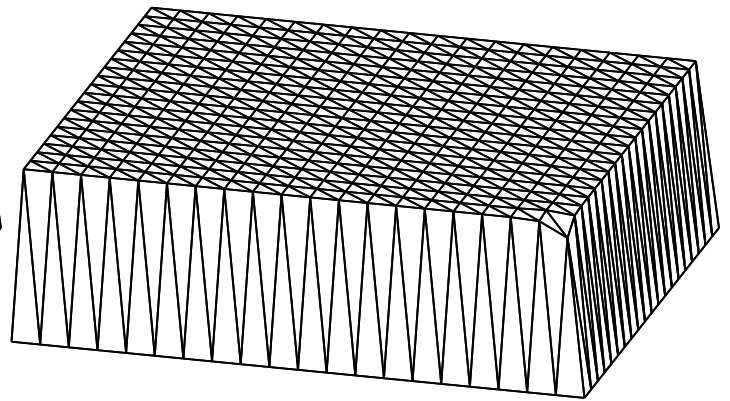


Figure 3: The present method cures the oscillations of the standard Galerkin solution. Piecewise bilinear ($Q1$) and linear ($P1$) elements are used.

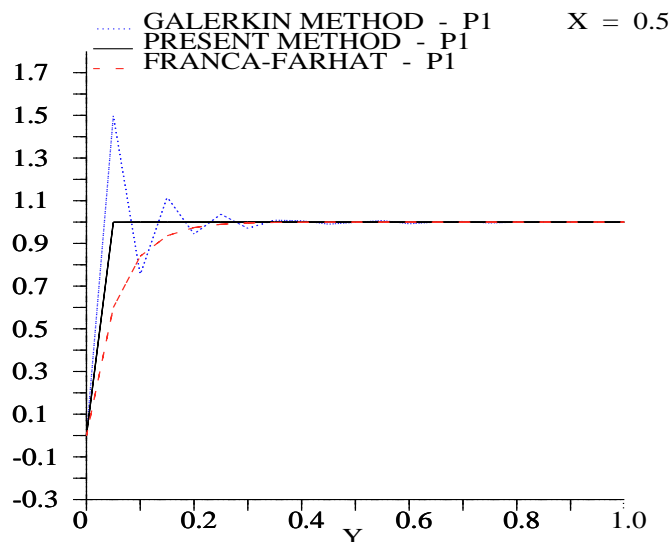
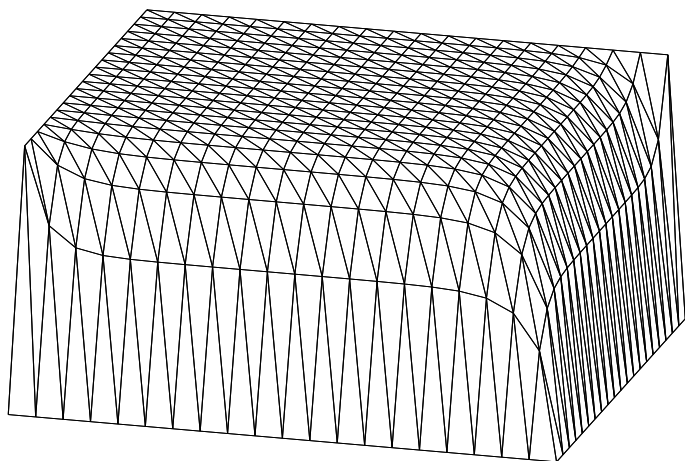


Figure 4: The present method is more accurate than the method proposed in [6].

4.2 Skew advection and the influence of reaction

We present two different sets of data for the problem of advection skew to the mesh using two different slopes and a uniform velocity field (see Figure 5 for the problem statement). In all simulations we impose $\nu = 10^{-4}$ and use 400 bilinear elements in a uniform mesh. We compare the Galerkin method with the present method gradually increasing the reactive coefficient σ as follows: 0, 10^{-2} , 10^{-1} , 1 and 10.

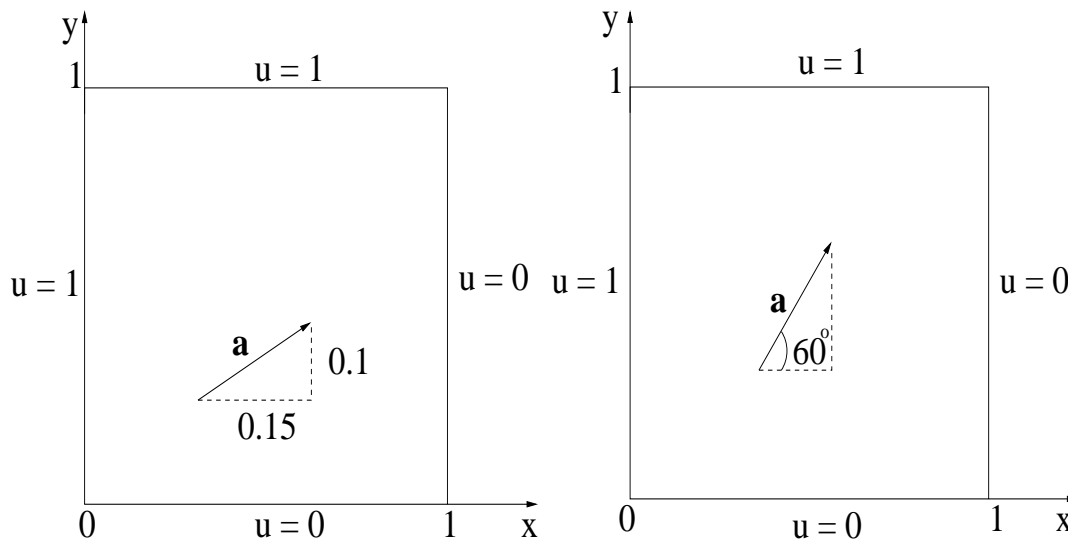


Figure 5: Domains for skew advection problems with two different convection fields.

In all cases the present method eliminates the oscillations with improved precision compared to the Galerkin method and to former versions of this method (figures 8-13), specially when the mesh parameter is computed as suggested by residual-free bubbles (see Figures 6 and 7). The comparison with the Franca-Farhat method is presented in Figure 11.

PRESENT METHOD - HARARI-HUGHES' h

PRESENT METHOD - RESIDUAL-FREE-BUBBLES h

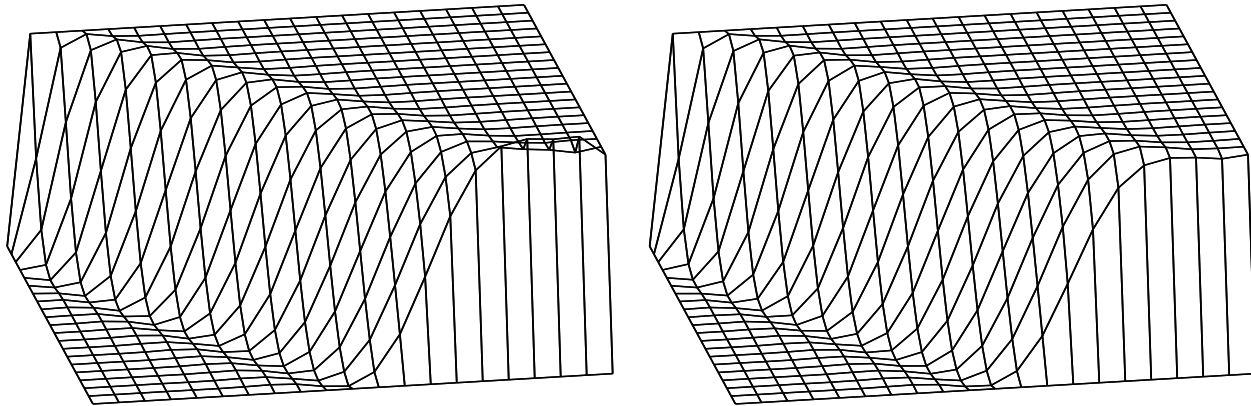


Figure 6: First skew advection problem. Comparison between the present method with the mesh parameter using Harari-Hughes' h [11] and residual-free-bubbles' h . Here $\sigma = 0$.

GALERKIN METHOD

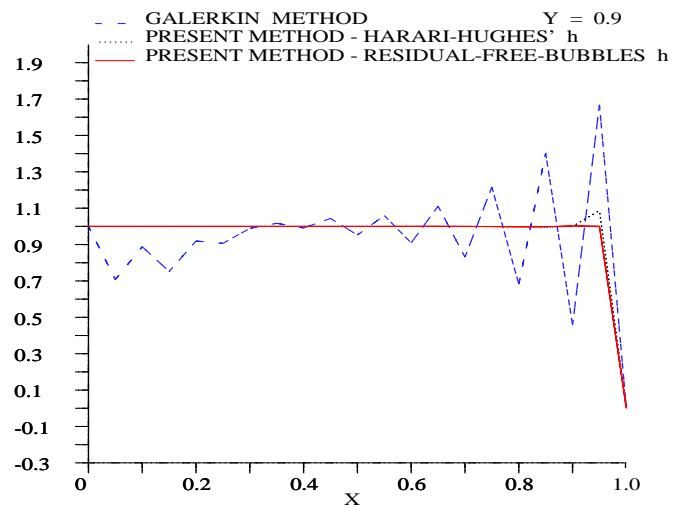
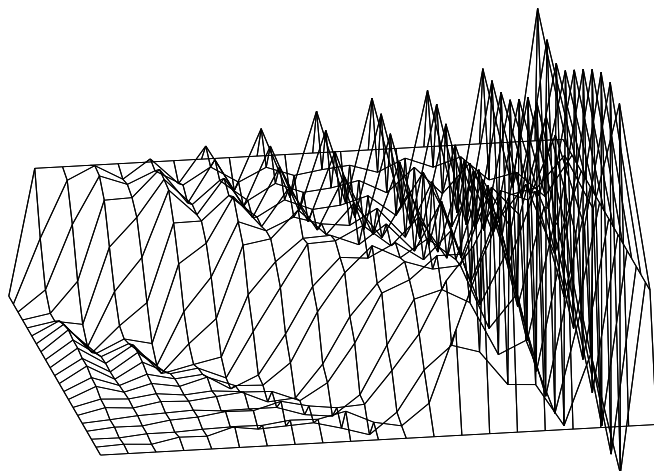


Figure 7: Solution using the Galerkin method when $\sigma = 0$. Comparison between the Galerkin method, and the present method with the mesh parameter using Harari-Hughes' h and residual-free-bubbles' h at $y = 0.9$. The second strategy corrects the oscillations on the boundary.

GALERKIN METHOD

PRESENT METHOD

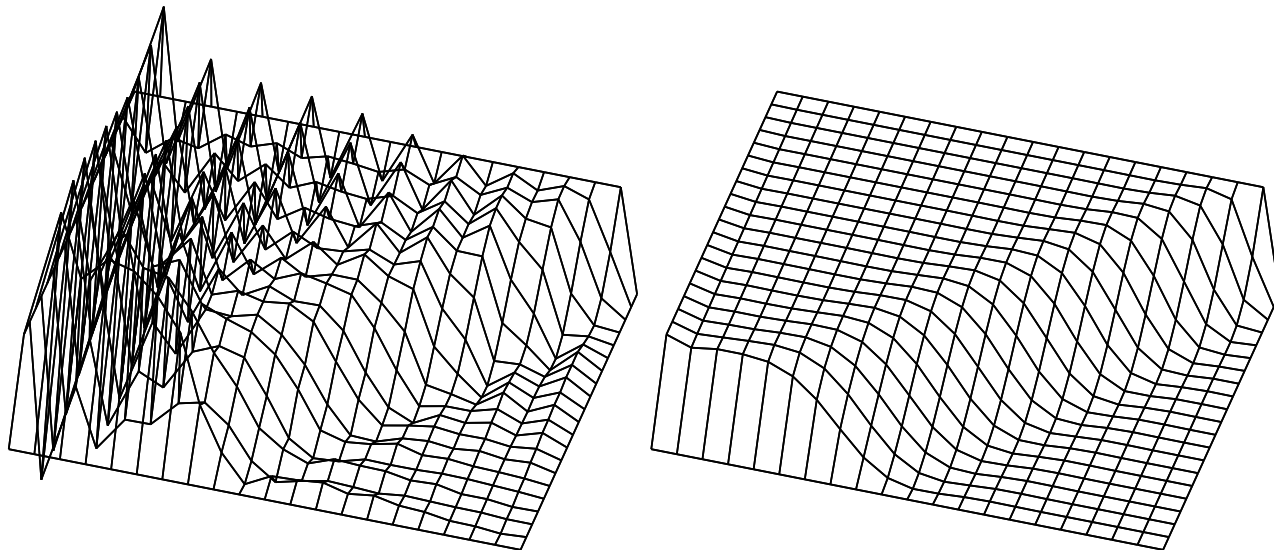


Figure 8: First skew advection problem. Comparison between the Galerkin method and the present method when $\sigma = 10^{-2}$.

GALERKIN METHOD

PRESENT METHOD

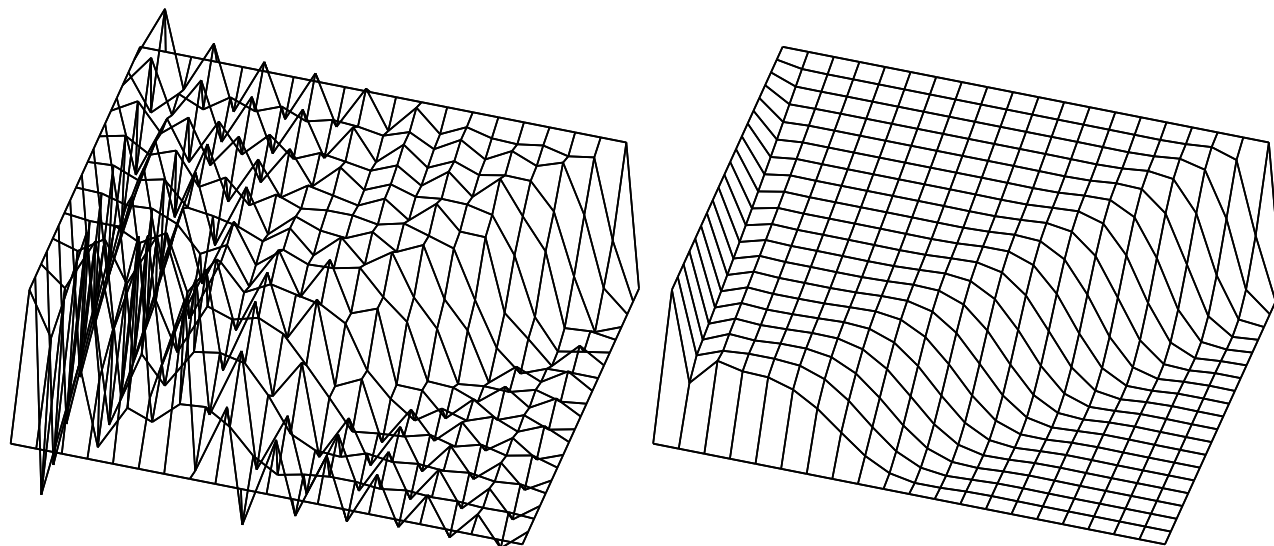


Figure 9: First skew advection problem. Comparison between the Galerkin method and the present method when $\sigma = 10^{-1}$.

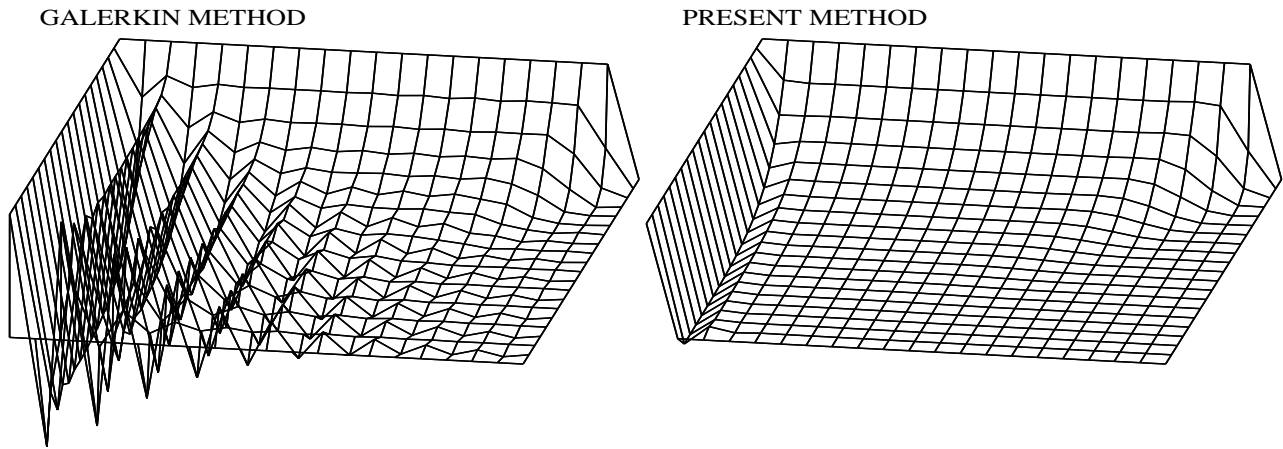


Figure 10: First skew advection problem. Comparison between the Galerkin method and the present method when $\sigma = 1$.

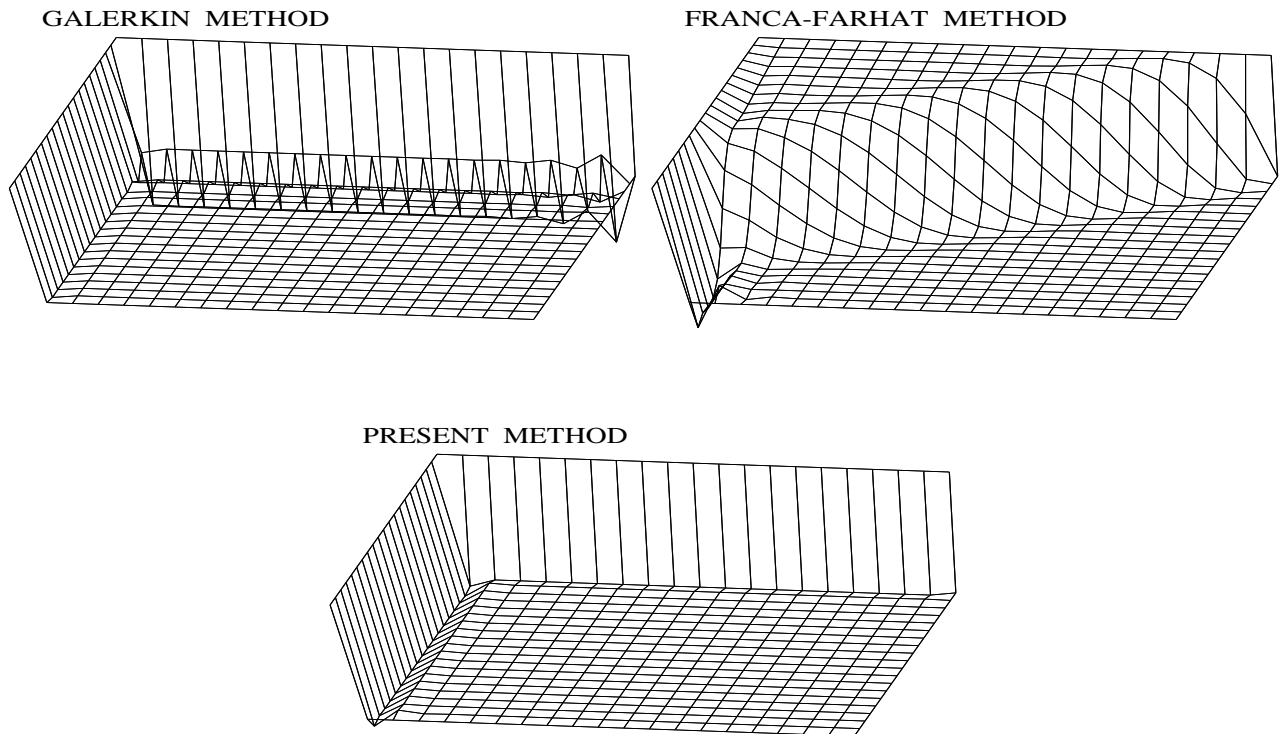


Figure 11: First skew advection problem. Comparison between the Galerkin method, the Franca-Farhat method and the present method when $\sigma = 10$.

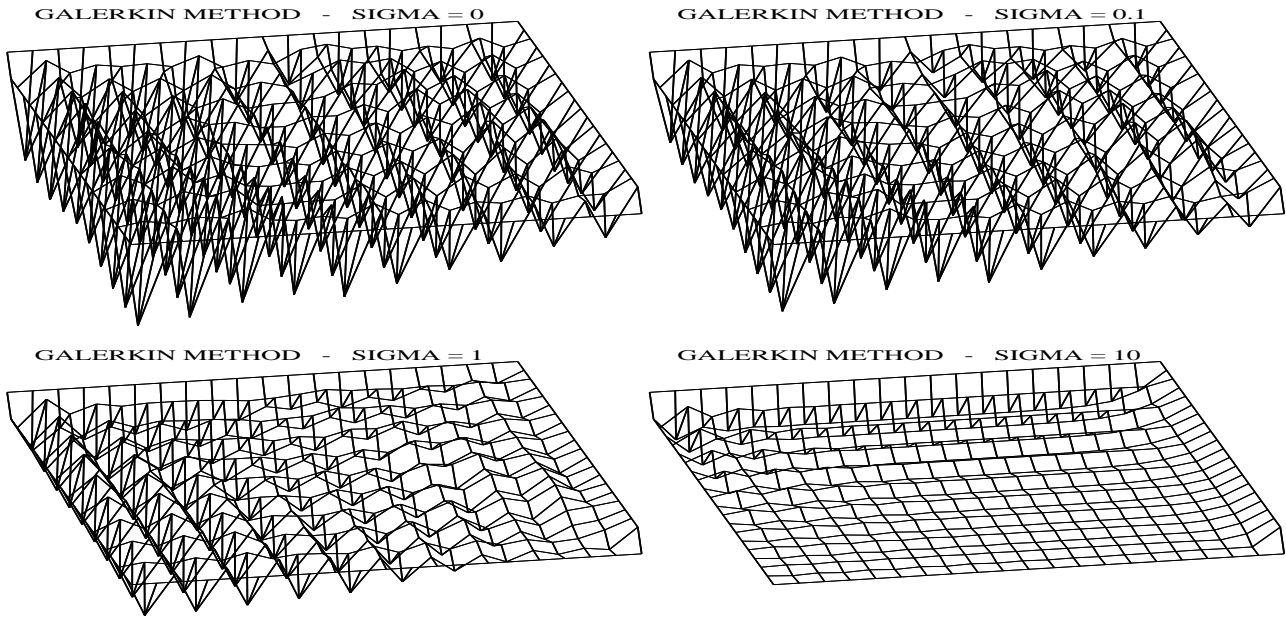


Figure 12: Second skew advection problem. Solutions by the Galerkin method with different σ values.

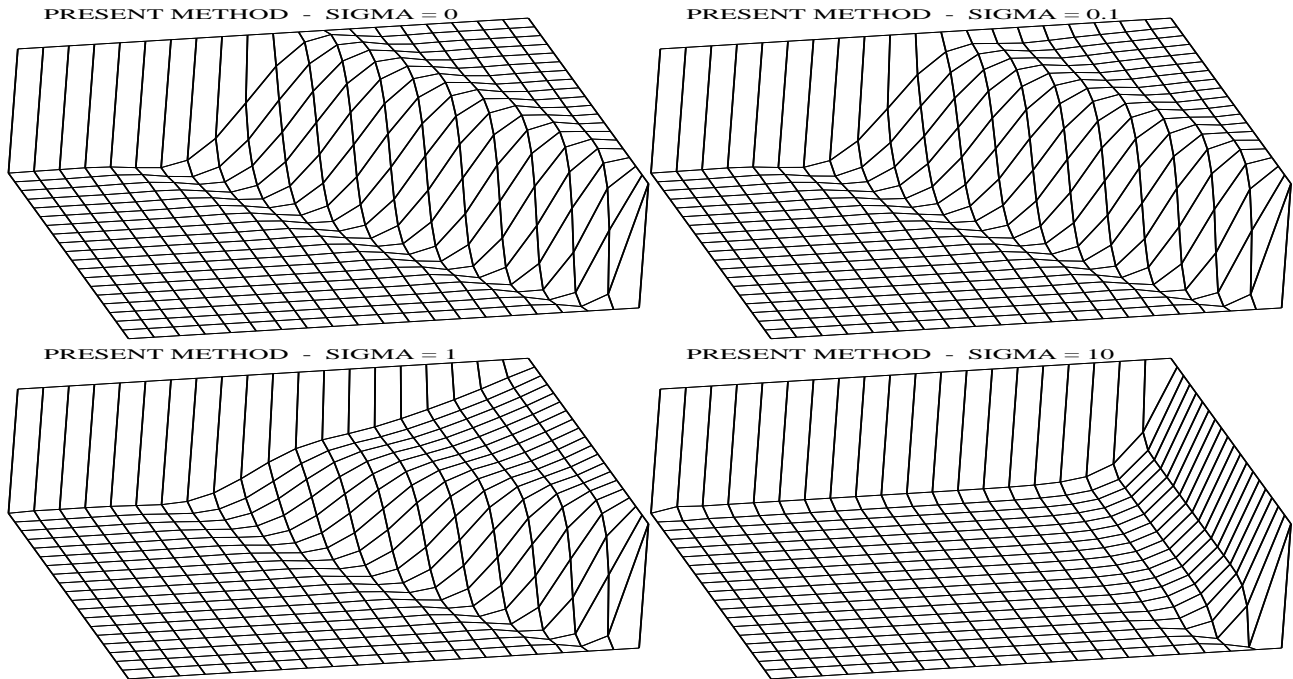


Figure 13: Second skew advection problem. Solutions by the present method with different σ values. The scale here is different to the figure 12.

4.3 Thermal boundary layer

Let us consider a rectangular domain subject to the boundary conditions presented in Figure 14. Here the advection field is given by $\mathbf{a} = (2y, 0)$ in Ω .

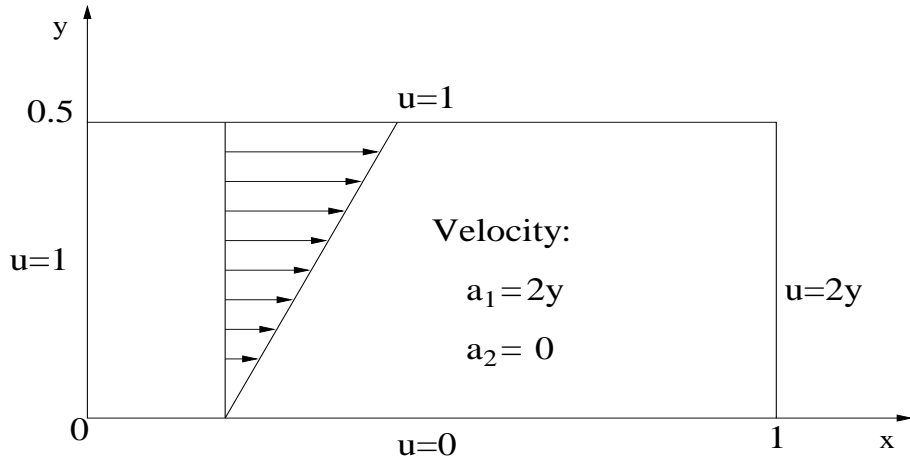
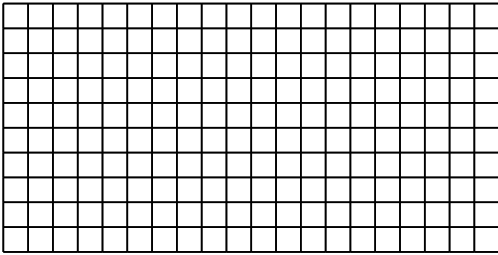


Figure 14: Problem statement for thermal boundary layer problem.

We wish to compare the present method using bilinear elements in uniform and non-uniform meshes. For the first mesh we used 200 elements and for the second one, 360 elements (see Figure 15).

HOMOGENEOUS MESH



NON-HOMOGENEOUS MESH

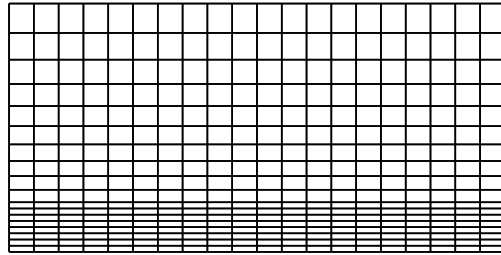


Figure 15: Different meshes used for the thermal boundary layer problem.

First we compare the different mesh parameter strategies using the second mesh (see Figures 16 and 17). The residual-free bubbles mesh h as defined in Figure 1,

yields a better performance than the computation using h as suggested by Harari and Hughes in [11].

In Figure 18 we note that both meshes yield similar results for the present method using the residual-free bubbles mesh parameter h and the Galerkin method yields oscillations for the same test when $\sigma = 0.5$. It is clear that the simple presence of the reactive term is not enough to dampen the oscillations in the Galerkin method.

PRESENT METHOD - HARARI-HUGHES' h

PRESENT METHOD - RESIDUAL-FREE-BUBBLES h

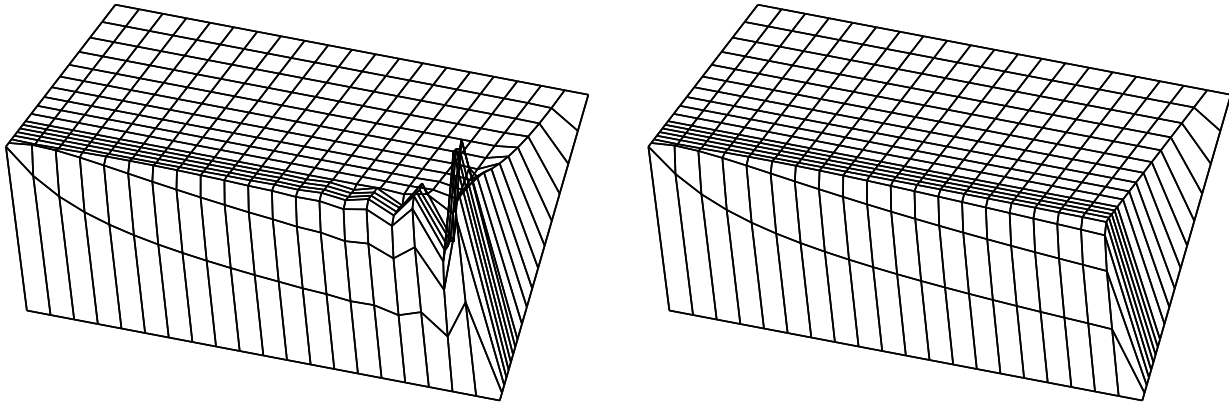


Figure 16: Comparison of different strategies for the h parameter calculation. $\sigma = 0$ and $\nu = 10^{-5}$. The parameter h from bubbles removes oscillations.

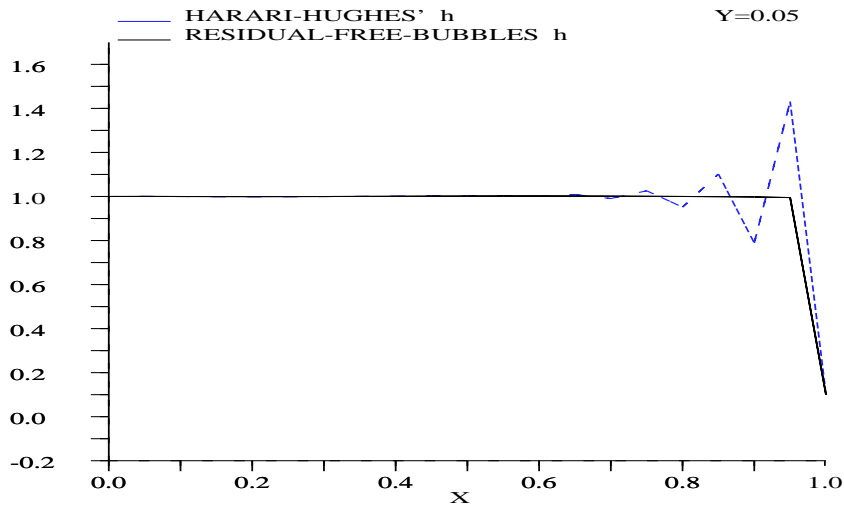
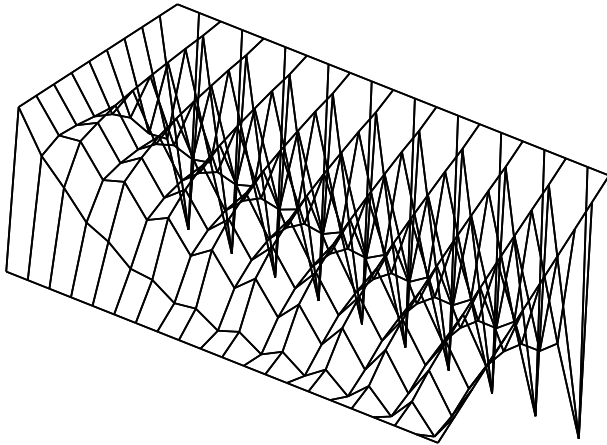
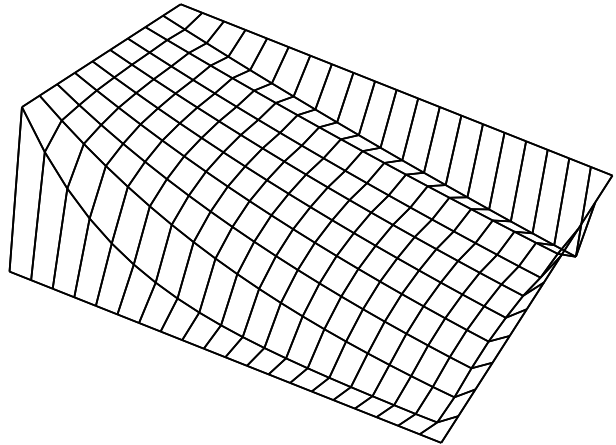


Figure 17: Solutions at $y = 0.05$ by the present method using different strategies for the h parameter.

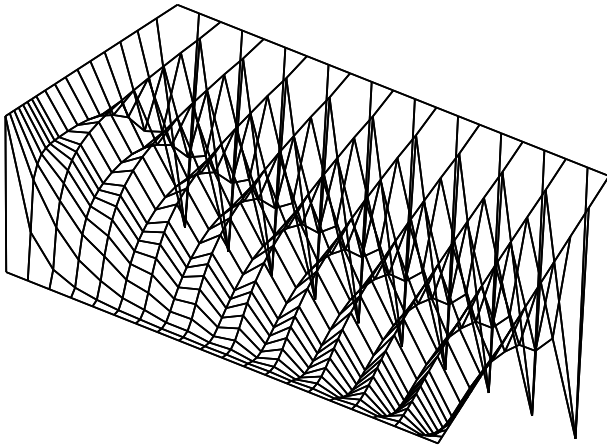
GALERKIN METHOD - HOMOGENEOUS MESH



PRESENT METHOD - HOMOGENEOUS MESH



GALERKIN METHOD - NON-HOMOGENEOUS MESH



PRESENT METHOD - NON-HOMOGENEOUS MESH

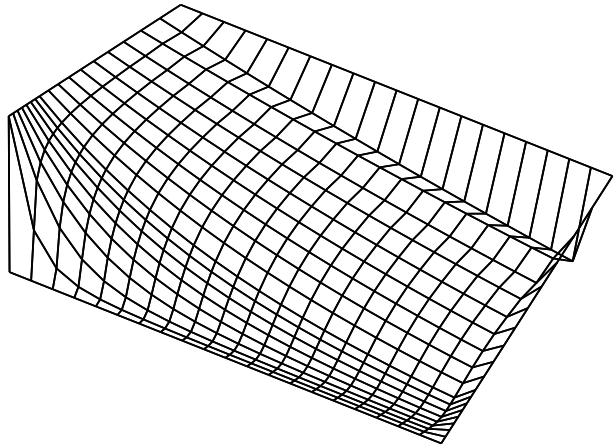


Figure 18: Comparison between the Galerkin method and the present method with $\sigma = 0.5$ and $\nu = 10^{-5}$ for different meshes.

4.4 NACA problem

We now consider a NACA problem using a non-uniform mesh with linear elements. This problem illustrates the ability of the present method to solve a complex problem, using the advection field which is the solution to the linearized Navier-Stokes problem (see Figure 19) with Reynolds number equal 10. The reaction's coefficient is $\sigma = 5$ and the diffusion's coefficient, $\nu = 10^{-5}$. A mesh with 6668 linear elements is employed (see Figure 20). Boundary conditions for the thermal problem are: specify the temperature at top, bottom and left side boundaries of the computational domain as $u = 0$ and on the surface of the NACA as $u = 1$; at the outflow boundary on the right side boundary a zero flux is prescribed.

We compare the contours for the Galerkin method versus the present method in Figure 21 and cuts of the solutions in Figure 22. We use a very fine mesh to calculate the solution with the Galerkin method, but it still presents spurious oscillations. The present method corrects most of those abnormalities, improving the accuracy of the solution.

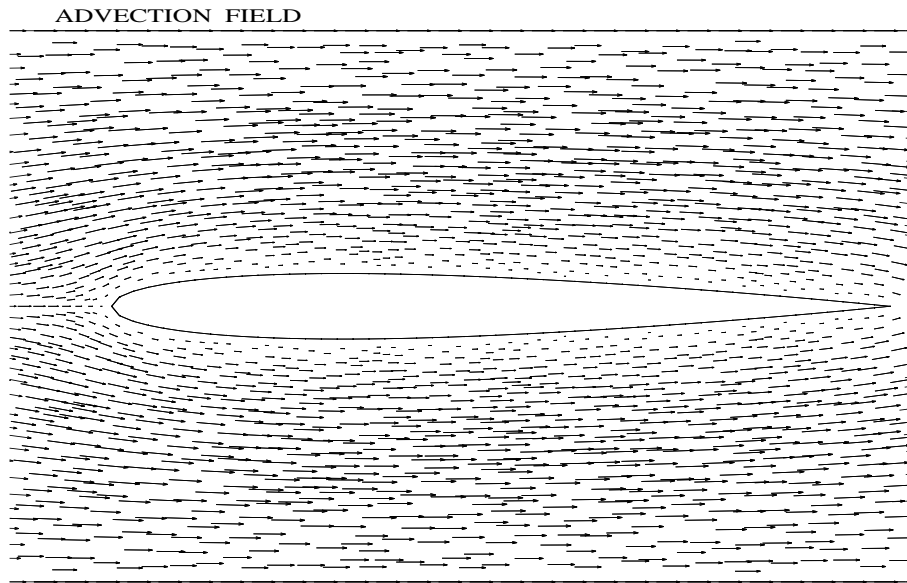


Figure 19: The convective field is the solution of a linearized Navier-Stokes problem.

MESH

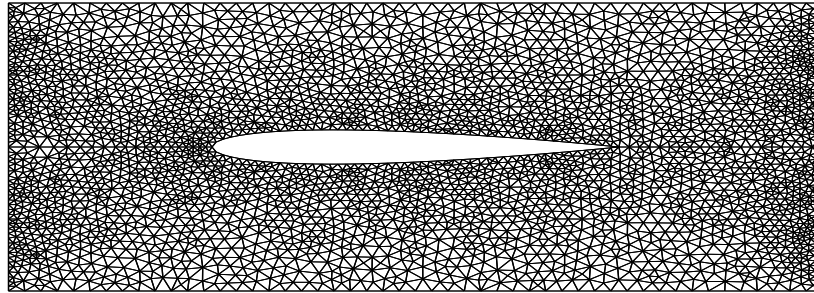
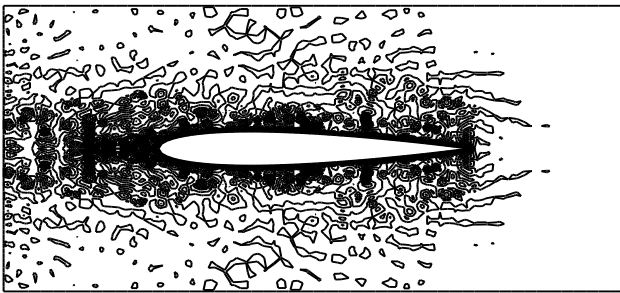


Figure 20: Mesh of the NACA problem.

GALERKIN METHOD



PRESENT METHOD

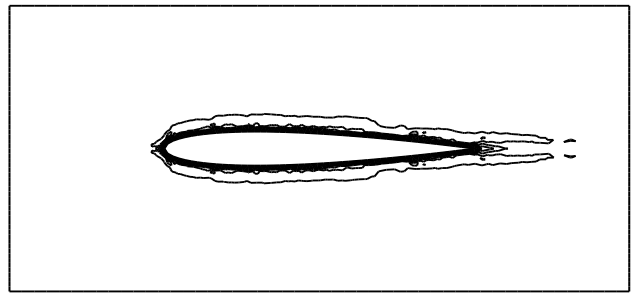


Figure 21: Contours of the Galerkin method and the present method: the present method improves the accuracy of the approximation.

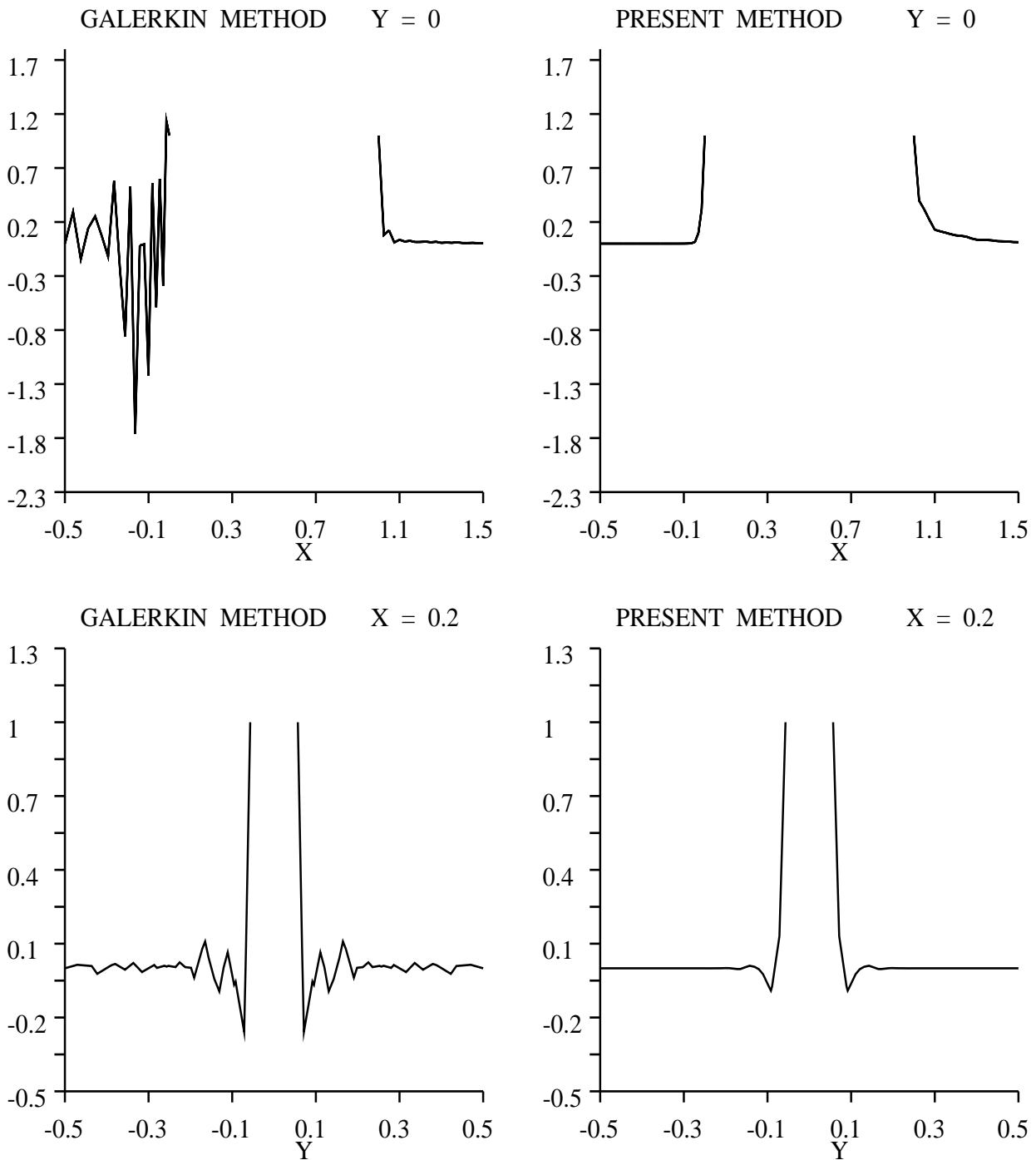


Figure 22: Comparison between the Galerkin method and the present method at cuts of the solutions at $y = 0$ and at $x = 0.2$. The oscillations in the Galerkin solution are corrected by the present method.

References

- [1] F. Brezzi, M.O. Bristeau, L.P. Franca, M. Mallet, and G. Rogé. A relationship between stabilized finite element methods and the Galerkin method with bubble functions. *Comput. Methods Appl. Mech. Engrg.*, 96:117–129, 1992.
- [2] F. Brezzi and A. Russo. Choosing bubbles for advection-diffusion problems. *Math. Models Meth. Appl. Sci.*, 4:571–587, 1994.
- [3] A. N. Brooks and T. J. R. Hughes. Streamline upwind/Petrov-Galerkin formulations for convection dominated flows with particular emphasis on the incompressible Navier-Stokes equations. *Comput. Methods Appl. Mech. Engrg.*, 32:199–259, 1982.
- [4] P.G. Ciarlet. *The Finite Element Method for Elliptic Problems*. North-Holland, Amsterdam, 1978.
- [5] R. Codina. Comparison of some finite element methods for solving the diffusion-convection-reaction equation. *Comput. Methods Appl. Mech. Engrg.*, 156:185–210, 1998.
- [6] L. P. Franca and C. Farhat. Bubble functions prompt unusual stabilized finite element methods. *Comput. Methods Appl. Mech. Engrg.*, 123:299–308, 1995.
- [7] L. P. Franca, S. L. Frey, and T. J. R. Hughes. Stabilized finite element methods: I. Application to the advective-diffusive model. *Comput. Methods Appl. Mech. Engrg.*, 95:253–276, 1992.
- [8] L. P. Franca, A. Nesliturk, and M. Stynes. On the stability of residual-free bubbles for convection-diffusion problems and their approximation by a two-level finite element method. *Comput. Methods Appl. Mech. Engrg.*, 166:35–49, 1998.
- [9] L. P. Franca and A. Russo. Deriving upwinding, mass lumping and selective reduced integration by residual-free bubbles. *Appl. Math. Letters*, 9:83–88, 1996.
- [10] I. Harari and T.J.R. Hughes. Finite element methods for the Helmholtz equation in an exterior domain: model problems. *Comput. Methods Appl. Mech. Engrg.*, 87:59–96, 1991.
- [11] I. Harari and T.J.R. Hughes. What are C and h ?: Inequalities for the analysis and design of finite element methods. *Comput. Methods Appl. Mech. Engrg.*, 97:157–192, 1992.
- [12] T. J. R. Hughes and A. Brooks. A multidimensional upwind scheme with no crosswind diffusion. In T. J. R. Hughes, editor, *Finite Element Methods for Convection Dominated Flows*, pages 19–35. ASME, 1979.
- [13] T. J. R. Hughes, L. P. Franca, and G. M. Hulbert. A new finite element formulation for computational fluid dynamics: VIII. The Galerkin-least-squares method for advective-diffusive equations. *Comput. Methods Appl. Mech. Engrg.*, 73:173–189, 1989.

- [14] J.C. Simo, F. Armero, and C.A. Taylor. Stable and time-dissipative finite element methods for the incompressible Navier-Stokes equations in advection dominated flows. *Int. J. Num. Meth. Eng.*, 38:1475–1506, 1995.